Microstructure and Properties of Pb Nanowires Fabricated by Casting

2008 Jpn. J. Appl. Phys. 47 4815

(http://iopscience.iop.org/1347-4065/47/6R/4815)

Japanese Journal of Applied Physics
Vol. 47, No. 6, 2008, pp. 4815–4819

Microstructure and Properties of Pb Nanowires Fabricated by Casting

Jung-Hsuan CHEN, Shen-Chuan LO[1,2], Chuen-Guang CHAO*, and Tzeng-Feng LIU

Department of Materials Science and Engineering, National Chiao Tung University, Hsinchu, Taiwan 300, Republic of China
[1]*Department of Microstructure and Characterization, Material and Chemical Research Laboratories, Industrial Technology Research Institute, Hsinchu, Taiwan 310, Republic of China*
[2]*Nanotechnology Research Center, Industrial Technology Research Institute, Hsinchu, Taiwan 310, Republic of China*

(Received October 26, 2007; accepted February 21, 2008; published online June 13, 2008)

In this study, we fabricated Pb nanowires in porous alumina membranes with different diameters by pressure casting. It can produce a large quantity of Pb nanowires with average diameters of 20, 80, 200, and 300 nm and lengths of up to 10 μm. The diameter and length of the nanowires can be controlled by selecting templates with a desired size. The microstructure and size effects of Pb wires on the solidification process were investigated by scanning electron microscopy (SEM), transmission electron microscopy (TEM), X-ray diffraction analysis (XRD), and thermal analysis. The nanowires with average diameters of 20 and 80 nm were single crystals, but those with average diameters of 200 and 300 nm were polycrystals. Finally, we also discussed the melting behaviors of the Pb nanowires in the porous alumina matrix. [DOI: 10.1143/JJAP.47.4815]

KEYWORDS: Pb nanowire, pressure injection, solidification, microstructure, size effect

1. Introduction

Casting is a type of material processing exploiting the fluidity of a liquid to pour into a prepared container and solidifying upon cooling. This process has been studied and applied in the scientific and industrial areas for several centuries. The knowledge and techniques of metal casting have been very widely researched. In casting, we need an appropriate mold material, which depends on the chemical characteristics of the substance under consideration, and on the required temperature. A porous alumina membrane is a type of ceramic material and has a low thermal conductivity to keep the solid-liquid interface solidified along a single direction. Since the porous alumina membrane has a high chemical stability and maintains its porous structure during heating and high-pressure processes, it is a very suitable mold.

As the ratio of the surface to volume is large in the case of nanostructure materials, it is possible to observe some distinctive properties of relative bulk materials. One-dimensional (1D) nanomaterials exhibit electronic,[1,2] magnetic,[3] optical,[4] physical, and chemical properties greatly differing from those observed in the corresponding bulk materials due to quantum effects. There are many synthetic approaches that have enabled the successful fabrication of definition high-quality 1D nanomaterials. Direct template filling is the most straightforward method in the preparation of nanowires and nanorods. Templates frequently used to fabricate nanowires include a porous alumina membrane, porous silicon, a polycarbonate membrane, and a zeolite film. In particular, a porous alumina membrane with hexagonally packed nanometer-sized channels has widely been used for more than 10 years.[5,6] By carefully choosing anodization conditions, the pore size, pore density, and channel length can be effectively controlled by anodizing pure aluminum films in various electrolytes. Metallic nanowires can also be synthesized by filling a porous alumina membrane with molten metals. It is interesting and useful to combine the traditional process with the nanotechnology. However, few studies have indicated the solidified behavior and structure of the nanowires in the aspect of nanoscale casting. In the present paper, we attempt to find the cause of the nanowires of high crystallinity and also describe the melting temperature of nanowires dependent on the size effect.

2. Experimental Procedure

To investigate the properties of the 1D quantum wire system, a template is usually used to fabricate various material nanowires. Porous anodic alumina membranes with average channel diameters of 20, 80, 200, and 300 nm were used as templates in this experiment. Aluminum foil (99.7 wt %) was annealed at 873 K for 2 h and then electropolished. After electropolishing, two-step anodization process progressed. The anodization for the 20 nm pore diameter template was performed at 18 V in the 10 wt % sulfuric acid (H_2SO_4). The 80 nm pore diameter template was fabricated by anodizing the Al substrate at 40 V in 0.3 M oxalic acid ($H_2C_2O_4$). The templates with the diameters of 200 and 300 nm were generated by anodizing a purity Al substrate at 160 V in the 10 wt % phosphoric acid electrolyte. The thicknesses and pore sizes of the templates were controlled under anodization conditions. Hexagonally ordered pores were obtained on the aluminum surface.

The fabrication of the Pb nanowires was based on the vacuum melting and pressure casting of melted metal. The purity of the initial lead was 99.99 wt %, while the content of impurities did not exceed 10^{-2} wt %. Then, a piece of Pb metal and an alumina template were placed inside the vacuum chamber in which the vacuum pressure was maintained at 10^{-6} Torr. A hydraulic force was applied to the Pb melt to inject the melt into the nanochannels of the porous alumina membrane. Solidification proceeded using a water cooling method at the bottom of the chamber. The Pb nanowires were formed after cooling to room temperature.

The morphologies and crystal structures of the Pb nanowires were characterized by scanning electron microscopy (SEM) and X-ray diffraction (XRD; D/max 25.50 V, Cu Kα radiation). The detailed microstructures of the Pb nanowires were observed by transmission electron microscopy (TEM). A PerkinElmer diamond differential scanning calorimeter (DSC) was used to measure the thermal characteristics of the Pb nanowires.

*E-mail address: cgchao@mail.nctu.edu.tw

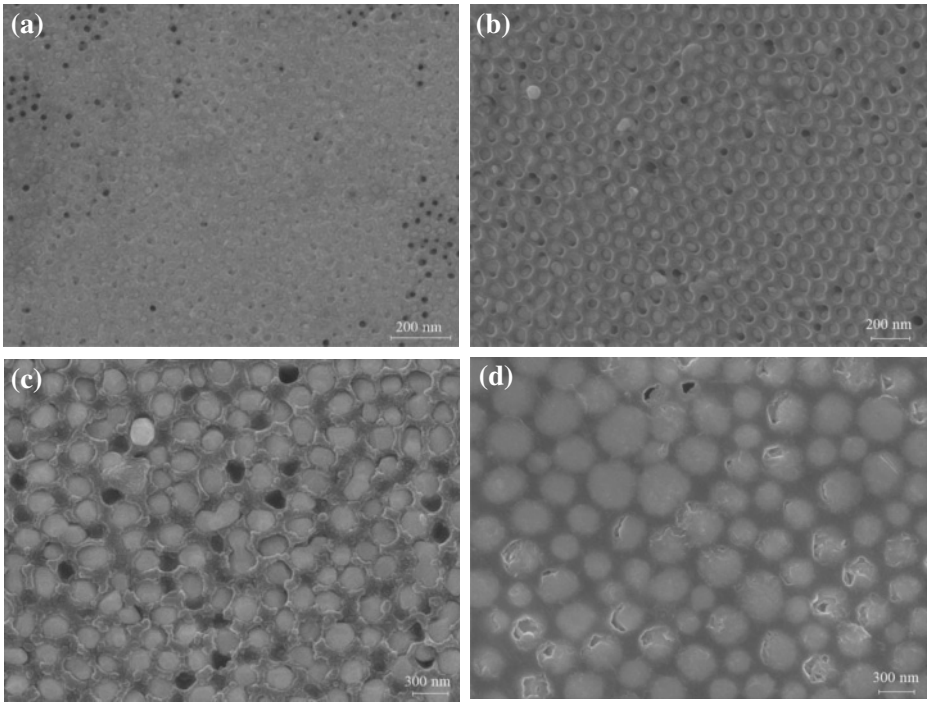

Fig. 1. SEM images of Pb nanowires with diameters of (a) 20, (b) 80, (c) 200, and (d) 300 nm.

3. Results and Discussion

During casting, the molten Pb metal was injected into the anodic alumina membrane forming metallic nanowires. The force required to inject Pb melt into the nanochanel is proportional to the surface tension of the melt. The pressure for melt injection into nanochannel can be evaluated as[7,8)]

$$\Delta P = \frac{F}{A} = -\frac{2\gamma\cos\theta}{r}, \tag{1}$$

where F is the normal force, A is the area of the specimen, r is the radius of the nanochannel, γ is the surface tension of Pb melt, and θ is the contact angle between the Pb melt and the porous alumina membrane. The surface tension of Pb melt is 468 dyne/cm and the contact angle assumes the least favorable case of complete nonwetting ($\theta = 180^\circ$). This is because most liquid metal/oxide systems have nonwetted ($\theta > 90^\circ$) and nonreactive wetted conditions. Moreover, the contact angles would be greater on a rough surface than on a corresponding flat surface.[9)] Therefore, the force required to inject the Pb melt into nanochannels with different diameters could be calculated.

After nanochannels were filled with the Pb melt, solidification proceeded immediately with the water cooling method. Heat loss from the bottom of the wire is often a sufficient heat sink. Solidification proceeds from the bottom of the wire to the top region in this experiment. Crystal growth is induced by the movement of the interface between the solid and the melt. When a metal solidified, it nucleates at a large number of points and consists of many crystals in conventional casting. Therefore, the growth of high-quality single crystals is difficult and requires a planar liquid-solid interface and a particularly solidified direction which is antiparallel to that of heat flow. That is, the formation of cells or dendrites must be avoided, and a sufficiently high thermal gradient or a sufficiently low growth rate leads to plane front growth. The temperature gradient at the interface is defined as

$$G = \frac{dT}{dz}. \tag{2}$$

It can be observed that the solid/liquid interface of a pure metal is always stable when the temperature gradient is positive ($G > 0$). The growth rate V means the movement rate of the solid/liquid interface. The ratio G/V largely determines solidification morphologies (planar, columnar, and dendritic). The product of G and V is equivalent to the cooling rate that controls the scale of the microstructures.[10,11)] In this experiment, it is assumed that the steady stable condition for the temperature gradient through the wire is applicable. The temperature difference between the top and bottom of the wire is about 500 K. The length of the wire is 10 μm and the total cooling time is 10 minutes. Therefore, G and V could be estimated to be 5×10^7 K/m and 1.67×10^{-8} m/s, respectively. Due to the high G/V ratio and the directional solidification opposite to the direction of heat flow, solidification with a planar interface could occur and the individual nanowires with different diameters are believed to be single crystal structures.

Figure 1 shows that the top views of Pb nanowires with the diameters of 20, 80, 200, and 300 nm fabricated by pressure casting exhibit uniform distributions and have high filling ratios. TEM images of nanowires with diameters of 20 and 80 nm are displayed in Figs. 2(a) and 2(b), respectively. The bright field image suggests a uniform and nonbranched wire structure. The inset shows the corresponding selective area electron diffraction (SAED) of the Pb nanowire. According to the index of the SAED, the nanowire is a single-crystal structure growing along the [110] direction. However, the TEM micrographs presented in Figs. 2(c) and

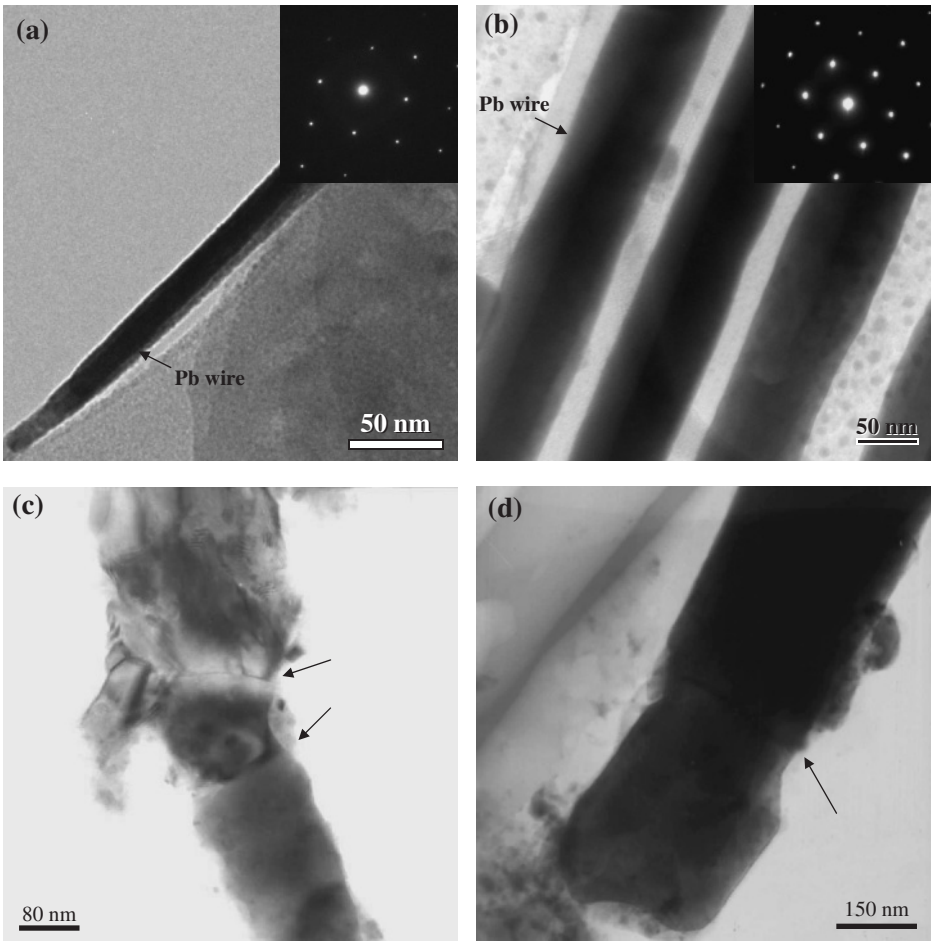

Fig. 2. TEM morphologies of Pb nanowires with diameters of (a) 20 and (b) 80 nm. The insets in (a) and (b) show the selective area electron diffraction pattern of the corresponding Pb wire. (c) and (d) show the TEM images of the Pb nanowires with diameters of 200 and 300 nm, respectively. Grain boundaries are indicated by arrows.

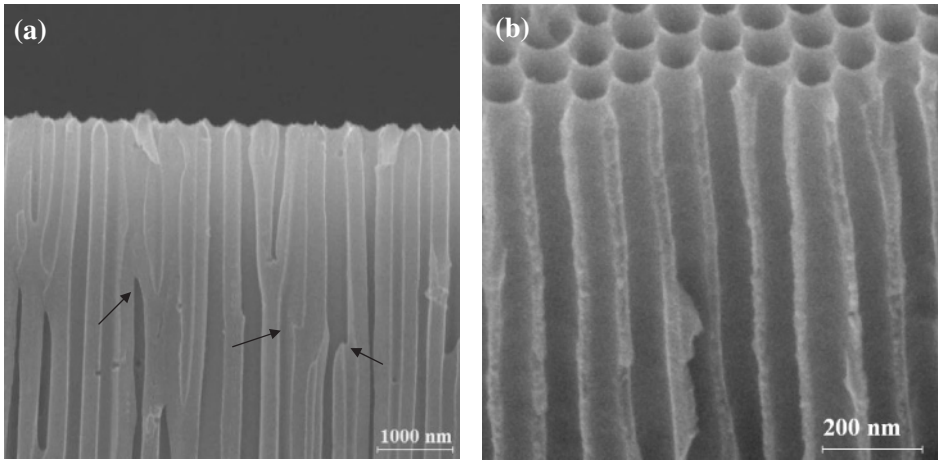

Fig. 3. Cross-sectional images of porous alumina membranes with pore sizes of about (a) 200 and (b) 80 nm.

2(d) show that interrupted wire structures, such as the grain boundary, appear when the diameters of the nanowires are 200 and 300 nm. During casting, the mold shape and material also affect the characteristics of the crystals, such as orientation, shape, composition, and perfection. The alumina membranes with pore diameters larger than 200 nm synthesized in the phosphoric acid solution have the less order and regular pore structures. The cross-sectional image of the alumina membrane with a diameter of 200 nm reveals the presence of some defects, such as branches, interrupted, and deformed channels, as shown in Fig. 3(a). The imperfect regions may induce a change in heat flow direction or offer preferably nucleated sites during solidification. Therefore, more polycrystals would possibly grow in these nanowires. Figure 3(b) shows the cross-sectional image of the alumina membrane whose pore diameter is 80 nm. Since the nanochannel is straight and uninterrupted, the wire solidified in it could form a single crystal structure, as shown in Fig. 2(b).

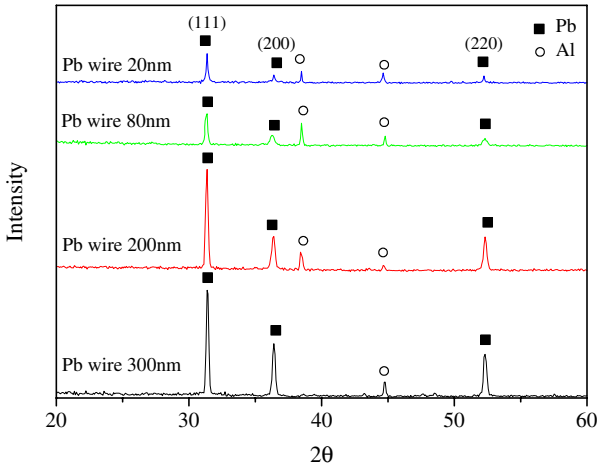

Fig. 4. (Color online) XRD spectra of Pb nanowires with 20, 80, 200, and 300 nm average diameters.

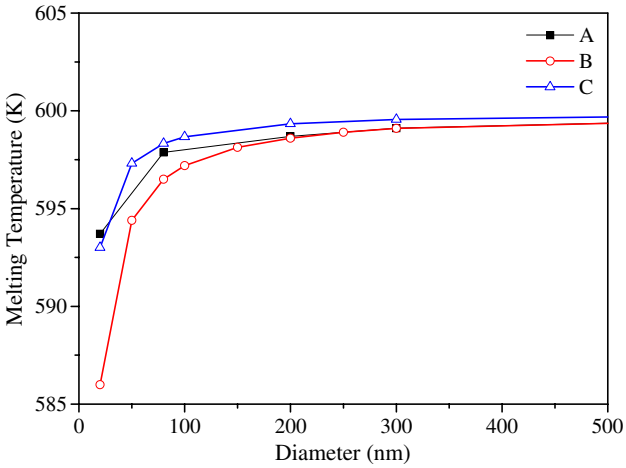

Fig. 5. (Color online) Relationship between melting temperature and Pb wire diameter. Curve A denotes experimental results for the melting temperatures of Pb nanowires. Curves B and C show theoretical predictions based on eqs. (3) and (4), respectively.

The results of the XRD analysis of Pb nanowires of four different wire diameters are shown in Fig. 4. Three peaks of the Pb nanowires identified as (111), (200), and (220) are the same as the peaks of Pb bulk with a face-centered cubic structure.[12,13] The major crystal plane of Pb nanowires with different diameters IS the (111) lattice plane. The relative line intensities of $I_{(200)}/I_{(111)}$ are estimated. The intensity ratio decreases as the Pb wire diameter decreases. It can be shown that the nanowires produced by pressure casting, particularly those with small diameters, have a high crystallinity and a preferred crystal orientation; moreover, the crystal structure of bulk is preserved in the nanowires after heating and high pressure processes.

As the size of nanomateris decreases, the number of surface atoms greatly increases. The large surface to volume ratio of nanomaterials could change the thermodynamic properties determined by the number of surface atoms. Since the reduced coordination number of the surface atoms increases the surface energy, atom diffusion occurs easily at low temperatures. To study the size effect on the melting temperature of the Pb nanowires in the porous alumina membrane, DSC analyses were carried out. Figure 5 shows the relationship between the melting temperature obtained by DSC measurement and the Pb nanowire diameter. Curve A denotes experimental values for Pb nanowires with diameters ranging from 20 to 300 nm. It can be seen that the melting temperature decreases apparently as the Pb nanowire diameter decreases.

Qi[14] has developed a model accounting for the melting temperature of free-standing nanosolids. For rod like nanosolids, such as nanowires, the relationship between the melting temperature and the wire diameter can be expressed as

$$T_{m(r)} = T_{mb}\left(1 - \frac{2d}{3r}\right). \tag{3}$$

Here, $T_{m(r)}$ and T_{mb} are respectively the melting temperatures of the nanowire with the radius r and the corresponding bulk material, and d is the atomic diameter. For the Pb metal, T_{mb} is 600 K and the atomic diameter is 0.35 nm.[15] The theoretically calculated results are shown in curve B.

For nanostructures embedded in a matrix, they can melt below the melting point of the bulk materials when the interfaces between the embedded nanocrystals and the matrix are incoherent.[16–18] Zhang *et al.*[16] reported that the $T_{m(r)}$ of metallic nanomaterials embedded in a matrix is described as

$$T_{m(r)} = T_{mb}\exp\left(-\frac{\alpha - 1}{r/r_0 - 1}\right). \tag{4}$$

Here, r_0 is the critical radius of a particle in which all atoms are located on its surface. α is defined as the ratio of the mean square displacement of atoms on the surface to that in the interior of crystals, as shown in

$$\alpha = \frac{\dfrac{(h_M/h_m)^2 T_{mb}}{T_{Mb}} + 1}{2}. \tag{5}$$

Here, h_M and h_m are respectively the atomic diameters of the matrix and the nanomaterials, and T_{Mb} is the melting point of the matrix. For Pb nanowires embeded in the alumina matrix, $r_0 = 0.7$ nm and $\alpha = 1.156$, the variation in $T_{m(r)}$ with diameter is presented as curve C in Fig. 5.

The experimental values (curve A) are in agreement with the results in curve B especially for the diameters larger than 200 nm. The melting temperature of free-standing Pb wires (curve B) decreases rapidly when the diameter is less than 50 nm. This result means the presence of the size effect in the free-standing Pb wires. Furthermore, the melting temperatures of the Pb wires with diameters less than 80 nm (curve A) are near the melt behavior of the Pb wires embedded in the alumina matrix (curve C). These results could be explained by considering the contribution of the free surface of the Pb wires with different diameters in the porous alumina membranes. In our experiment, the Pb wires with diameters of 200 or 300 nm show a larger free surface fraction than the wires with diameters less than 80 nm. Therefore, the thermal properties of the Pb wires in the alumina membrane are similar to those of the free-standing wires with larger diameters. When the diameter decreases, the melting temperature variation shows the same tendency with the wires embedded in the matrix.

4. Conclusions

Pb nanowires with diameters of 20, 80, 200, and 300 nm are successfully fabricated by casting. A Pb melt is solidified along the reversed direction of heat flow from the bottom to the top for the wire inside an alumina membrane. The nanowires bear a high temperature gradient and have a low growth rate besides directional solidification. According to theoretical calculations, the nanowires prepared by pressure casting are single crystal structures regardless of their diameters. From TEM experiments, as the diameters of the nanowires increase, the microstructures of the nanowires are easily formed polycrystals due to the effects of mold properties. In DSC analyses, the Pb nanowires in the alumina membrane exhibit a reduced melting temperature from the bulk. The size-dependent melting temperatures of the Pb nanowires in the porous alumina membrane are predicated by two models.

Acknowledgements

This work was supported by the National Science Council of the Republic of China under the Research Contract No. NSC95-2221 E009-062.

1) Y. Huang, X. Duan, Y. Gui, and C. M. Lieber: Nano Lett. **2** (2002) 101.
2) X. Duan, Y. Huang, Y. Gui, J. Wang, and C. M. Lieber: Nature **409** (2001) 66.
3) H. Pettersson, L. Bååth, N. Carlsson, W. Seifert, and L. Samuelson: Appl. Phys. Lett. **79** (2001) 78.
4) J. C. Johnson, H. Yan, R. D. Schaller, P. B. Petersen, P. Yang, and R. J. Saykally: Nano Lett. **2** (2002) 279.
5) S. Shingubara: J. Nanopart. Res. **5** (2003) 17.
6) Y. T. Pang, G. W. Meng, L. D. Zhang, Y. Qin, X. Y. Gao, A. W. Zhao, and Q. Fang: Adv. Funct. Mater. **12** (2002) 719.
7) Z. Zhang, J. Y. Ying, and M. S. Dresselhaus: J. Mater. Res. **13** (1998) 1745.
8) C. C. Chen, Y. Bisrat, Z. P. Luo, R. E. Schaak, C. G. Chao, and D. C. Lagoudas: Nanotechnology **17** (2006) 367.
9) C. W. Extrand: Langmuir **18** (2002) 7991.
10) M. C. Flemings: *Solidification Processing* (McGraw-Hill, New York, 1974).
11) W. Kurz and D. J. Fisher: *Fundamentals of Solidification* (Trans Tech Publication, 1992).
12) P. Villars and L. D. Calvert: *Pearson's Handbook of Crystallographic Data* (Materials Information Society, 1991).
13) JCPDS No. 04-0686.
14) W. H. Qi: Physica B **368** (2005) 46.
15) B. B. Alchagirov, A. G. Mozgovoy, and Kh. B. Khokonov: High Temp. **41** (2003) 755.
16) Z. Zhang, J. C. Li, and Q. Jiang: J. Phys. D **33** (2000) 2653.
17) X. W. Wang, G. T. Fei, K. Zheng, Z. Jin, and L. D. Zhang: Appl. Phys. Lett. **88** (2006) 173114.
18) Q. Jiang, X. H. Zhou, and Z. Wen: Appl. Surf. Sci. **195** (2002) 38.